Endoplasmic reticulum stress activates autophagy but not the proteasome in neuronal cells - implications for Alzheimer's disease

Wiep Scheper, Diana A.T. Nijholt, Tjitske R. de Graaf, Rob Zwart, Frank Baas, Elise S van Haastert, Jeroen J.M. Hoozemans, Celia R. Berkers, Huib Ovaa, Ana Osório Oliviera

Endoplasmic reticulum stress activates autophagy but not the proteasome in neuronal cells – *implications for Alzheimer's disease.*

Running title: ER stress and proteolysis in Alzheimer's disease

Diana A.T. Nijholt[1], Tjitske R. de Graaf[1], Elise S. van Haastert[2], Ana Osório Oliviera[1], Celia R. Berkers[3], Rob Zwart[1], Huib Ovaa[3], Frank Baas[1,4], Jeroen J. M. Hoozemans[2] and Wiep Scheper*[,1,4]

[1]Neurogenetics Laboratory, Academic Medical Center, University of Amsterdam, Amsterdam, The Netherlands

[2]Department of Pathology, VU University Medical Center, Amsterdam, The Netherlands

[3]Division of Cell Biology, The Netherlands Cancer Institute, Amsterdam, The Netherlands

[4]Department of Neurology, Academic Medical Center, University of Amsterdam, Amsterdam, The Netherlands

***Correspondending author**

W. Scheper

Neurogenetics laboratory

Academic Medical Center

P.O.Box 22660

1100 DE Amsterdam

The Netherlands

T: +31-20-5664959

F: +31-20-5669312

E: w.scheper@amc.uva.nl

Abstract

Protein folding stress in the endoplasmic reticulum (ER) may lead to activation of the unfolded protein response (UPR), aimed to restore cellular homeostasis via transcriptional and post-transcriptional mechanisms. ER stress is also reported to activate the ER overload response (EOR), which activates transcription via NF-κB. We previously demonstrated that UPR activation is an early event in pre-tangle neurons in Alzheimer's disease (AD) brain. Mis- and unfolded proteins are degraded via the ubiquitin proteasome system (UPS) or autophagy. UPR activation is found in AD neurons displaying both early UPS pathology and autophagic pathology. Here we investigate whether activation of the UPR and/or EOR is employed to enhance the proteolytic capacity of neuronal cells. Expression of the immunoproteasome subunits β2i and β5i is increased in AD brain. However, the expression of the proteasome subunits is not increased by the UPR or EOR. UPR activation does not relocalize the proteasome or increase overall proteasome activity. Therefore proteasomal degradation is not increased by ER stress. In contrast, UPR activation enhances autophagy and LC3 levels are increased in neurons displaying UPR activation in AD brain. Our data suggest that autophagy is the major degradational pathway following UPR activation in neuronal cells and indicate a connection between UPR activation and autophagic pathology in AD brain.

Keywords: Alzheimer's disease, unfolded protein response, ubiquitin proteasome system, autophagy

Abbreviations: AD: Alzheimer's disease. HD: Huntington's disease. ER: Endoplasmic reticulum. UPR: Unfolded protein response. EOR: ER overload response. UPS: Ubiquitin proteasome system. NFT: Neurofibrillary tangle. Aβ: Amyloid beta. ERAD: ER associated degradation. GVD: granulovacuolar degeneration.

Introduction

The Alzheimer's disease (AD) brain is characterized by the accumulation of extracellular plaques composed of Amyloid beta (Aβ) and intracellular neurofibrillary tangles (NFTs) composed of hyperphosphorylated tau.[1] One of the early events in AD is activation of the unfolded protein response (UPR). We have previously shown that the UPR is activated in AD neurons that contain diffusely distributed hyperphosphorylated tau.[2] The UPR is a cellular stress response that is activated upon the accumulation of mis- or unfolded proteins in the endoplasmic reticulum (ER).[2,3] This response is aimed at restoring homeostasis by activating a number of responses that attenuate protein translation in general and promote transcription and translation of a number of genes involved in ER protein folding and degradation. Another, less well studied, ER stress response is the ER overload response (EOR), which is thought to be activated by the accumulation of proteins in the ER membrane and signals via NF-κB.[4,5]

Misfolded or defective proteins need to be degraded in order to ensure cell survival. The degradation of misfolded or defective ER proteins is mediated by a process termed ER associated degradation (ERAD).[6] Activation of the UPR induces the upregulation of a number of ERAD related genes, primarily via signalling through inositol requiring enzyme (Ire) 1α.[7] ERAD involves export of the misfolded proteins via specific export channels in the ER membrane, after which the proteins become targeted for degradation by the cytosolar ubiquitin proteasome system (UPS).[6] The UPS is a major degradational system in the cell that apart from degradation of misfolded proteins is involved in the degradation of short-lived proteins. The proteasome 20S catalytic core is comprised of three catalytically active beta (β) type subunits, β1, -2 and -5 which convey peptidyl-glutamyl peptide-hydrolyzing- (PGPH), trypsin- and chymotrypsin-like activity. The constitutive β subunits can be exchanged for the immuno subunits β1i, -2i and -5i under the influence of γIFN mediated NF-κB signalling, a phenomenon observed for example during

antigen presentation.[8] The immunoproteasome displays slightly altered catalytic activity for certain substrates, for example it is capable of degrading the tau protein faster and more efficient *in vitro.*[9] Changes in proteasome proteolytic activity are reported for several neurodegenerative disorders, including AD[10,11] and Parkinson's disease (PD).[12] Systemic administration of proteasome inhibitors to rats causes a PD-like phenotype, with α-synuclein and ubiquitin positive inclusion bodies and neurodegeneration in the substantia nigra.[12] This suggests that dysfunction of the UPS can lead to neurodegeneration. Interestingly, an increase in immunoreactivity to the immunoproteasome subunit β1i was observed in the AD brain[13], a change in proteasome subunit composition that is associated with increased chymotryptic activity.[13,14] This could be a response to the accumulation of substrates that require a different proteolytic specificity in order to be degraded.

Another major degradational system that has been reported to be activated by ER stress *in vitro* is autophagy.[15-17] Autophagy is involved in the degradation of long-lived proteins, organelles and aggregated proteins. During autophagy a double membrane is wrapped around the organelle or aggregate to be degraded and this autophagosome subsequently fuses with a lysosome, forming an autophagolysosome where degradation takes place. Autophagy is important for maintaining cellular homeostasis and is involved in neurodegenerative disorders. Mice that are deficient for autophagin (atg) 5[18] or atg7[19] accumulate ubiquitin positive cytoplasmic aggregates and show neurodegeneration. Healthy neurons only rarely show autophagosomes or autolysosomes, whereas large amounts of autophagic vacuoles can be observed in AD neuronal cell bodies and dystrophic neurites.[20] A commonly observed lesion in the AD brain is granulovacuolar degeneration (GVD), which is thought to be a disturbed autophagic process.[21] It is typically seen in the cytoplasm of the pyramidal neurons of the cornu ammonis (CA) 1 and subiculum of the hippocampus, sites that also show extensive tau pathology.[2] GVD consists of

electron-dense granules surrounded by a clear vacuole that measure 2 – 4 μM in size. The presence of GVD in this region of the hippocampus correlates well with the diagnosis of AD.

The UPR is activated as an early response in neurons in AD. Activation of the UPR may be a signal to enhance the degradational capacity of the affected neuron. Both the UPS and autophagy play a role in the degradation of aberrant proteins in neurodegenerative disorders and have been implicated in AD. Neurons in the AD hippocampus that are positive for UPR markers are associated with early UPS pathology, in the form of ubiquitin positive, p62 negative inclusion bodies, and show autophagic pathology in the form of GVD.[2] In this study we investigate the role of these two degradational systems during ER stress *in vitro* and in human AD brain material. All hypopheses that are tested in this study are visualized in Figure 8a.

Results

Immunoproteasome subunit expression is increased in the AD brain

First we evaluated expression of the immunoproteasome subunits β2i and β5i in AD hippocampus using immunohistochemistry. We previously reported that UPR activation is predominantly observed in AD hippocampus and is present in neurons associated with GVD.[2,3] Therefore immunoreactivity to the β2i and β5i subunits was assessed in this region of a cohort of AD and age matched non-demented controls. Both β2i and β5i expression is seen in AD and control hippocampus and based on morphological assessment is observed in neurons, glial cells and endothelial cells (Figure 1a-l). Increased reactivity to the β1i subunit in AD and aged hippocampus was previously described by Mishto *et al.*[13] and was also observed in these cell types. Here we show a granular pattern of β2i reactivity in neurons, of which the intensity is increased in high Braak stages for neurofibrillary changes (predominantly Braak stage IV-VI). No clear association is observed between β2i immunoreactivity in neurons and the local presence of Aβ plaques and neurofibrillary changes (data not shown). A moderate increase in β5i immunoreactivity in neurons is observed in high Braak stages. However, there is a remarkable increase in the number of glial cells that are immunoreactive for β5i in Braak stages II-VI. To confirm that β5i is predominantly expressed in glial cells we performed double immunolabelling using β5i combined with a marker for astrocytes (GFAP) or for microglia (Iba1). These doublestainings show that β5i is expressed in astrocytes and microglia (Figure 1m-n).

Our data show that expression of the immunoproteasome subunits is increased in the AD hippocampus. We have previously demonstrated that ER stress markers can be readily observed in the AD hippocampus in neurons that contain hyperphosphorylated tau which has not precipitated into a tangle.[2] As the UPR is aimed at restoring ER homeostasis and is known

to promote ERAD, we next investigated whether UPR activation is responsible for the increased expression of the immunoproteasome in an *in vitro* model.

ER stress: Effects on proteasome subunit expression

We investigated the effect of ER stress on proteasome subunit expression via quantitative PCR (qPCR) and Western blot analysis. Tunicamycin (Tm) was used to chemically induce an ER stress response which results in activation of the UPR. Differentiated neuronal SK-N-SH cells were treated with increasing concentrations of Tm followed by assessment of mRNA and protein levels of proteasome subunits and UPR responsive genes. No change in mRNA levels of the catalytically inactive α subunits HC5 and C7 or the catalytically active constitutive β subunits β1, -2 and -5 is observed after induction of ER stress (Figure 2a). Figure 2b shows the UPR is active under these conditions as mRNA levels of the UPR responsive genes BiP and CHOP are increased 25.0 fold +/- 5.5 and 18.8 fold +/- 2.4, respectively. ER stress increases expression of the immuno subunits β5i (alternative transcript β5i-1: 3.9 fold +/- 0.4 and β5i-2: 4.1 fold +/- 0.7) and to a lesser extent β2i (2.0 fold +/- 0.3). As a positive control for induction of the immuno β subunits γIFN was used and results in upregulation of these genes (5.9 fold +/- 0.6, 132.0 fold +/- 22.5; and 576.8 fold +/- 81.3 for β2i, β5i-1 and β5i-2, respectively). No regulation of the UPR responsive genes by γIFN is observed. The β1i immuno subunit is increased by γIFN but is below the detection limit under control or Tm conditions in our model and therefore not included in Figure 2a. Our data show ER stress results in a moderate upregulation of the immuno β subunit mRNA levels compared to their classical activator γIFN (Figure 2a and b).

Specific antibodies were used to assay the protein levels of the immunoproteasome subunits β2i and β5i and the constitutive subunit β2. In accordance with our qPCR data γIFN results in increased expression of β2i and β5i (~35 fold), but not of β2. We find no regulation of the proteasome subunits β2i, β5i and β2 by Tm. The increase in BiP levels (~3 fold) indicates that

the UPR is active under these conditions[3] (Figure 2). To exclude effects of different kinetics, we extended the Tm treatment to 48 hrs, but this did not change the outcome of the experiments (data not shown). Combined, we find moderate upregulation of the immunoproteasome subunits β2i and β5i at the mRNA level during ER stress, but this does not lead to a change at the protein level.

ER stress does not affect β2i promoter activity

Most genes that are subject to direct regulation via the UPR contain ER stress responsive elements (ERSEs) in their promoter sequence. No ERSEs are found in the immuno β subunit proximal promoters, but all contain a consensus NF-κB site that is expected to be activated by the EOR if it is functional (Figure 3a). In order to directly investigate immunoproteasome β subunit promoter NF-κB responsiveness and the effect of ER stress on promoter activity, we cloned the promoter of β2i upstream of the luciferase gene. The β2i subunit is upregulated in AD post mortem material (Figure 1), is upregulated by γIFN in our qPCR and Western blot experiments (Figure 2) and contains a consensus NF-κB binding site (Figure 3a). Hek293 cells were transfected with the β2i promoter-luciferase construct and treated with γIFN or Tm for 16 h. The BiP promoter-luciferase construct was used as a control for induction of the UPR.[22] Activity of the β2i promoter is increased (~2 fold) by γIFN but, as expected, there is no change in BiP promoter activity because it does not contain an NF-κB element (Figure 3b). Abolishment of the β2i NF-κB binding site by site-directed mutagenesis prevents γIFN mediated regulation, demonstrating that the β2i promoter is responsive to NF-κB and that the NF-κB signalling route is functional in this model. In contrast, ER stress induced by Tm has no effect on β2i promoter activity, but does increase BiP promoter activity (Figure 3b), again demonstrating an active UPR. Although β5i promoter responsiveness was not directly investigated, combined with our Western blot data, our experiments indicate that expression of the immunoproteasome β subunits is not regulated by the UPR or EOR pathways of the ER stress response.

ER stress has no effect on β5i subunit localization

Several studies have indicated an enrichment of the immunoproteasome at the smooth ER membrane[23,24] which may facilitate rapid degradation of un- or misfolded proteins exported out of the ER by ERAD. Relocalization in response to a stimulus may therefore present another level of regulation in addition to effects on expression. We investigated localization of the β5i subunit in differentiated SK-N-SH cells under conditions of ER stress. Because the great majority of β subunits is incorporated in proteasome complexes, this is a good reflection of subunits in actual proteasomes.[25] Cells were double-stained using antibodies directed against the β5i proteasome subunit and calnexin, an integral ER membrane protein (Figure 4). Reactivity to β5i and its colocalization with calnexin is increased by γIFN, indicating that the increased β5i protein localizes at least in part to the ER membrane. Treatment with Tm does not result in any change in the β5i intensity level confirming our Western blot data (Figure 2c). In addition, the localization of β5i is not affected by activation of the UPR. Although increased immunoreactivity to β2i and β5i is observed in AD, our *in vitro* studies suggest UPR activation is not responsible for this induction.

ER stress does not increase proteasome activity

During ER stress the demand for proteolytic activity is increased and UPR activation increases the expression of several genes involved in ERAD, the system that targets misfolded proteins in the ER for degradation by the proteasome. We show that the proteasome β subunits are not subject to this classical ER stress responsive regulation (Figures 2 and 3), nor is relocalization to the ER observed (Figure 4). However, this does not exclude regulation of the proteolytic activity of the proteasome. Using an unstable fluorescent substrate a small decrease in proteasome activity was previously observed under conditions of ER stress.[26] This reporter system has the disadvantage that it depends on more factors than proteasome activity alone (e.g. transcription and translation). This method could yield inaccurate results, especially during ER stress, when

translation in general is inhibited. In order to directly investigate the effect of ER stress on total proteasome activity a fluorescent proteasome activity probe was used that covalently binds the catalytic subunits of active proteasomes.[27] Differentiated neuronal SK-N-SH cells were treated with Tm and subsequently incubated with the fluorescent reporter. Subunits were separated using SDS-PAGE and the fluorescent signal for each band was visualized (Figure 5a) and quantified (Figure 5b). Under basal conditions we find no detectable activity of the immunoproteasome; corroborating our expression data. ER stress has little to no effect on proteasome activity in our cell model. A decrease in activity is observed at the highest concentration of Tm used however this may be caused by Tm induced toxicity.

Our data show that there is no upregulation of the UPS by the UPR during ER stress. Because during ER stress there is an increased presence of misfolded proteins, this may lead to accumulation and toxicity if they are not degraded. To investigate this, we treated neuronal cells with different types of ER stress inducers (Tm, thapsigargin (Th) and 2-deoxyglucose (2DG)) and observe that this does not result in the accumulation of polyubiquitinated proteins in these cells (Figure 6a, upper panel), in contrast to the massive accumulation observed when using proteasome inhibition. This may imply that the proteasome is redundant during ER stress, but it cannot be excluded that basal proteasome activity is still sufficient to deal with the misfolded protein load during ER stress. If this is the case, complete inhibition of proteasome activity should induce a massive ER stress response. Using an ER stress reporter as well as the endogenous BiP response[28] we have previously demonstrated that proteasome inhibition does not induce a robust ER stress response, suggesting that proteasomal activity is dispensable to resolve ER stress under conditions of UPR activation.

ER stress was previously shown to be able to induce autophagy *in vitro*[15,29] and we subsequently investigate whether this is the preferred route for degradation of proteins during ER stress and UPR activation.

LC3 processing is increased during ER stress

In order to determine whether ER stress increases autophagy in our cell model we measured LC3-II levels induced by various ER stressors (Figure 6a, middle panel). LC3-II is a good marker for autophagy as the amount of LC3-II is directly correlated with the amount of autophagosomes.[30] As expected, Tm, Th and 2DG increase LC3-II levels; indicating that autophagy becomes more active under conditions of ER stress. Figure 6b shows the LC3-II/LC3-I ratio as determined from Figure 6a. An increased ratio compared to the control situation is indicative of an increase in activity of the autophagy pathway.

In the AD brain disturbed autophagic processes (e.g. the accumulation of autophagic vacuoles in dystrophic neurites and GVD in the neuronal soma) are commonly observed and we next investigated the expression of LC3 in the AD brain.

LC3 levels are increased in pPERK positive neurons in the AD brain

To investigate the autophagy pathway during AD immunohistochemistry was used to evaluate total levels of the autophagy marker LC3 in AD hippocampus. LC3 reactivity is abundant in hippocampal neurons in AD (Figure 7a) and control subjects (data not shown), whereas low intensity is observed in non-neuronal cells. The intensity of reactivity to LC3 is increased in AD in neurons showing GVD (Figure 7b and c). The staining of LC3 is observed throughout the cell body, but appears more intense at the edges of the vacuoles, corroborating that GVD is related to autophagosomes. Occasionally, reactivity with the granular material inside the vacuole is observed. We have previously shown that the UPR activation markers are associated with GVD

in the AD hippocampus[2,3] and we performed double immunohistochemistry to investigate the connection between LC3 and UPR activation. Phosphorylated PERK (pPERK) was used as a marker of an active UPR and, as expected in view of the close correlation of UPR and GVD observed previously, we find LC3 intensity is higher in neurons displaying pPERK reactivity (Figure 7d). These data show a clear correlation between activation of the UPR and the autophagy marker LC3 in human AD hippocampus. This corroborates our *in vitro* data demonstrating that the UPR preferentially activates the autophagy pathway and indicates that this response also occurs *in vivo*.

Discussion

In this study we investigated the effects of ER stress on the two major degradational systems in the cell; the UPS and the autophagy pathway, and their relation to AD. We found that neither the UPR nor the EOR is responsible for the induction of the immunoproteasome subunits in the AD hippocampus, nor does UPR activation influence proteasome localization or enhance its activity. However, we found that the UPR preferentially enhances autophagic degradation in response to ER stress (Figure 8).

The EOR was first reported in 1992. In this initial study a viral transmembrane protein that is retained in the ER induced a robust NF-κB response in Hek293 cells.[4] Another study indicated that the chemical ER stress inducers tunicamycin, thapsigargin and 2-deoxyglucose also elicit a NF-κB response.[5] However, in our study we found no ER stress mediated regulation of the NF-κB responsive subunits of the immunoproteasome in Hek293 or neuronal SK-N-SH cells. A small transcriptional response to ER stress was observed, however this was not sufficient to result in increased protein levels. As the immuno subunits were responsive to their classical activator γIFN, but were not stimulated by ER stress, this indicates that the EOR is not effective in our models. The discrepancy with previous studies might result from differences in the experimental approaches used. In our promoter activity experiments we made use of the endogenous β2i promoter that contains a single NF-κB responsive element whereas in the previous work a construct that contains five NF-κB binding sites was employed. A small induction of NF-κB may thus lead to increased activity of this NF-κB reporter construct, whereas induction of the endogenous β2i promoter will have a higher threshold for transcriptional activation and is unlikely to reach the level required to yield changes at the protein level. In addition, the earlier studies did not investigate the protein levels of endogenous NF-κB targets,

as was done in our study where we found a transcriptional response that did not result in changes at the protein level.

Increased expression of the immunoproteasome has been found in several neurodegenerative diseases, including AD (Figure 1 and Mishto *et al*.[13]), Huntington's disease (HD)[31] and amyotrophic lateral sclerosis (ALS).[32] Increased expression of β2i and β5i has been observed in affected brain areas of HD patients and in the HD94 mouse model[31], as well as in the spinal cord of an ALS mutant SOD1 mouse model.[32] Strikingly, effects that were observed in patient material and mouse models could not be recapitulated in a HD cell model[33], suggesting that a non-cell autonomous mechanism is responsible for this induction. In analogy to this, we found that NF-κB is not activated by the EOR in neuronal cells. Apart from an increase in the AD brain, an age dependent increase in the immunoproteasome was found. Reactivity to the β1i subunit was almost absent in young brain, whereas it was readily detectable in old brain.[13] Inflammatory markers were increased in the elderly brain compared to the young brain, providing support for an immune mediated increase of the immunoproteasome.[34] The occurrence of inflammatory responses in neurodegenerative disorders is well described in literature. In the AD brain a myriad of immune responses can be observed associated with Aβ deposits, including activation of complement, increased levels of proinflammatory cytokines (e.g. IL-1β, IL-6 and TNF-α) and activated glia.[35] Increased NF-κB activation was observed in neurons and glia associated with Aβ plaques.[36] The increased presence of Aβ and proinflammatory cytokines is likely to lead to a local increase in expression of the immunoproteasome in neuronal and non-neuronal cells.

Our data showed intense β2i immunoreactivity in AD pyramidal neurons, but less for β5i, whereas both subunits were expressed in glial cells. The β5i subunit is encoded within the major histocompatibility class (MHC) II locus on chromosome 6, whereas β2i is encoded on chromosome 16 (UCSC Genome Bioinformatics website). Neurons express low levels of MHC-II

and it is possible that this locus is transcriptionally less active in these cells, explaining the low β5i expression levels that we observed. Even though we were unable to link the UPR or the EOR to increased expression of the immunoproteasome, this does not rule out a protective effect of the immunoproteasome when it is present. The immunoproteasome is capable of degrading tau more efficiently and with fewer intermediate fragments.[9] Increased immunoproteasome levels may therefore attenuate tau aggregation and the formation of undegradable aggregates.

Like other neurodegenerative disorders that are characterized by the accumulation of mis- and unfolded proteins, decreased proteasome activity has also been reported in AD.[10,11] Although total proteasome content remains unchanged, a decrease in the PGPH- and chymotrypsin-like activity was measured using fluorigenic substrates incubated with brain lysates from AD affected areas.[10,11] This decrease was no longer observed when proteasome complexes were purified, instead a slight increase in chymotrypsin and trypsin-like activity was observed.[37] Aggregates have been shown to impair proteasome function, for example Aβ inhibits UPS dependent degradation *in vitro*[38] and removal of these aggregates by proteasome purification probably restores proteasome function. The increase in proteasome activity might be due to induction of the immunoproteasome under the influence of inflammatory mediators. Whether a decrease or blockage of proteasome activity is an early contributor to the pathology or caused by the disease process is not clear. Using a direct assay to study proteasome activity we demonstrated that UPR activation does not increase proteasome activity in our neuronal SK-N-SH cell model. A moderate decrease in proteasome activity, as measured by the accumulation of a fluorescently labelled UPS substrate, was previously described in MelJuso and Hela cell lines during chemically induced ER stress.[26] Because global translation is attenuated during ER stress, our activity probe assay gives a more direct and therefore more reliable result. The decrease in activity that we observed at higher ER stress levels is in accordance with the UPS substrate

data. This may indicate that ER stress contributes to decreased proteasome activity in the AD brain. However, caution is warranted as under these conditions toxic side-effects may obscure the data.

Combined, our experiments showed that in contrast to the increased expression of ERAD components through the Ire1α pathway of the UPR, UPR activation does not enhance proteasomal capacity *in vitro*. However, ER stress conditions are characterized by the accumulation of proteins in the ER which need to be degraded in order to ensure cell survival. The observation that ubiquitinated proteins do not accumulate during ER stress suggests that efficient degradation is taking place. We have previously shown that inhibition of the proteasome does not induce a robust ER stress response, as would be expected if the UPS plays a prominent role in degrading these proteins.[28] This appears to contradict studies that show that proteasome inhibition induces cancer cell apoptosis via ER stress. Fast dividing cancer cells are dependent on the proteasome for cell cycle progression and it is possible that this makes them more susceptible to proteasome inhibition and ER stress compared to non-dividing neuronal cells.

From literature it is known that ER stress can activate autophagy, as was demonstrated in yeast[15] and in neuronal cells.[16] Conversion of LC3-I to LC3-II is a good marker for the amount of autophagosomes present in the cell[30] and in agreement with these reports we found that ER stress increases the LC3-II/LC3-I ratio indicating autophagy becomes more active.[16] However, this ER stress mediated increase in LC3-II has only been demonstrated *in vitro* and we were interested in evaluating the expression levels of LC3 in the AD brain. Our immunohistochemical data demonstrated intense LC3 reactivity in pyramidal neurons in both AD and non-demented controls, indicating an important role for autophagy in neurons in the human brain. This is in line with observations showing that levels of LC3-I and LC3-II are high in the mouse brain compared

to other tissues.[39] It was long thought that autophagy was relatively inactive in neurons, however, in autophagy deficient mice it was demonstrated that basal autophagy is necessary to prevent neurodegeneration and that disruption of autophagy causes the accumulation of polyubiquitinated proteins in neurons in the mouse brain.[18,19] The finding that ubiquitin is not only involved in targeting substrates to the UPS but is also involved in selective autophagy, supports this hypothesis. For example, the Parkinson's disease associated ubiquitin ligase parkin is involved in ubiquitin mediated targeting of substrates to the autophagosomal/lysosomal pathway.[40]

High LC3 levels might be indicative of a highly active autophagy system and a priming of these cells to deal with misfolded proteins via autophagy. However, our antibody recognized both LC3-I and -II and thus did not give information about the autophagic state in these cells. Alternatively, high LC3 levels might be indicative of a disturbed autophagic state, in which LC3 accumulates because it cannot be degraded. Strikingly, we found high LC3 levels in neurons that show disturbed autophagic processes, demonstrated by the presence of GVD, and had activated the UPR. In addition to morphological observations of disturbed autophagy in AD[20], the levels of the upstream autophagic protein Beclin-1 are decreased in AD brain,[41] therefore different lines of evidence point to an impairment of autophagy in AD neurons. Our data indicate a direct link between UPR activation, autophagy and the occurrence of autophagic pathology *in vivo*.

Classically the ERAD pathway is reported to be the route by which misfolded or defective proteins exit the ER to be degraded by the proteasome.[6] If mis- and unfolded proteins accumulate to such an extent that the UPR is induced, the ERAD process might be overwhelmed. In addition, higher amounts of misfolded proteins in the ER may more readily form aggregates which cannot be exported into the cytoplasm. Under these conditions bulk degradation of parts of the ER containing these misfolded proteins may be a more favourable

pathway to restore homeostasis. This hypothesis is supported by the fact that ER stress markers are observed in GVD in AD and that these neurons display high levels of the autophagy marker LC3. It remains to be determined whether autophagic pathology arises because the autophagy system becomes overwhelmed by the increase in substrates or whether, with age or other events, the autophagic system becomes less efficient.

Our data support a model where the proteasome degrades misfolded proteins from the ER, but if this system is overloaded, either because the misfolding increases or because the proteasomal capacity is insufficient, autophagy is activated. This intricate regulation implies that autophagy is the major degradational pathway during activation of the UPR in neuronal cells. Figure 8 shows a diagram of all hypotheses tested in this study and the final model which shows that autophagy is activated by ER stress in neuronal cells. Because the UPR is activated in early Braak stages for tau pathology and in neurons in which the tau protein is not aggregated into tangles, it will be interesting to investigate this pathway as a target for early therapeutic intervention in AD.

Conflict of interest

The authors declare no conflict of interest.

Acknowledgements

Human brain tissue was supplied by the Netherlands Brain Bank. This study was supported by Internationale Stichting Alzheimer Onderzoek Nederland (ISAO #07506) and the Netherlands Organisation for Scientific Research (NWO). We thank Lisette Schmidt for initial experiments and Line De Kimpe and Hyung Elfrink for stimulating discussions.

Materials and Methods

Cell culture, differentiation and treatment. Human SK-N-SH neuroblastoma and HEK293 cells were cultured in Dulbecco's modified Eagle's medium with GlutaMAX (Gibco BRL, USA) supplemented with 10% fetal calf serum (FCS, Gibco BRL, USA), and 100 U/ml penicillin (Yamanouchi Pharma BV, The Netherlands). SK-N-SH cells were differentiated in culture medium supplemented with all *trans*-retinoic acid (Sigma, USA) in a final concentration of 10 μM for 5 days. Differentiated cells were treated with 500 U/ml γIFN (PBL Biomedical Laboratories, USA), epoxomycin, tunicamycin, thapsigargin and 2-deoxyglucose (all Sigma, USA) at indicated concentrations for 16 h.

RNA isolation and cDNA synthesis. For RNA isolation differentiated SK-N-SH cells ($5x10^5$/well in a 6-well plate) were harvested in TRIzol reagent (Invitrogen, USA) and total RNA was isolated using the QIAcube (QIAGEN, The Netherlands). The protocol used was according to the manufacturer's specifications. RNA concentrations and purity were assessed by OD measurements at 260 and 280 nm on a NanoDrop spectrophotometer (Thermo scientific, USA). For cDNA synthesis, 1μg of RNA and 125 pmol OligodT12 primer were dissolved in a total of 10 μl H_2O and incubated at 72°C for 10 min. Reverse transcriptase (RT) mix was added consisting of 5 μl 5x first strand buffer (Invitrogen, USA), 0.5 μl SuperScript II RNA polymerase (Invitrogen, USA), 10 mM dNTPs and 25 mM $MgCl_2$ in a total of 15 μl H_20. The mixture was incubated at 42°C for 1 h followed by 15 min at 70°C. cDNA quality was assessed on 0.8% agarose gel.

Real-time quantitative PCR. Real-time quantitative PCR (qPCR) was performed using the Light Cycler 480 system (Roche Applied Science, USA). Oligonucleotide primers (Sigma, USA) used for qPCR are listed in Table 1. Reaction volumes of 5 μl contained cDNA, 0.1 μM Universal Probe Library probe (Roche Applied Science, USA) also listed in Table 1, 0.4 μM forward

primer, 0.4 µM reverse primer and 2.5 µl 2x LightCycler 480 Probes Master (Roche Applied Science, USA). After denaturation for 10 min at 95°C, amplification was performed using 35 cycles of denaturation (95°C for 10 s), followed by annealing (58°C for 15 s), and elongation (72°C for 15 s). Results were analyzed using the LightCycler 480 software (Roche Applied Science, USA) version 1.5.

Table 1 Primers and probes used for qPCR 480 Light Cycler. Probe numbers refer to numbers in the Roche universal probe library.

Gene	**Primers (5' – 3')**	**Product size (bp)**	**Probe #**
HC5 (PSMB1)	FW: gggtcttaccagagagactcctt RV: gctccacattctgcatgttc	105	#19
C7 (PSMB2)	FW: cctcgaccgatactacacacc RV: caggatgaagcgtttctgg	73	#25
β1 (PSMB6)	FW: ggcggctaccttactagctg RV: aaactgcacggccatgata	124	#48
β2 (PSMB7)	FW: tgataagttgccttatgtcacca RV: ggcctaaacttatcttcaaatacagc	75	#36
β5 (PSMB5)	FW: catgatctgtggctgggata RV:ttcccttcactgtccacgta	60	#81
β1i (PSMB9)	FW: tcccaggttggaaaccagt RV: tcaaactccactgccatgat	140	#89
β2i (PSMB10)	FW: ggttccagccgaacatga RV: gcccaggtcacccaagat	83	#31
β5i variant 1, (PSMB8.1)	FW: ccctacccacccctgttt RV: cacccagggactggaaga	69	#1
β5i variant 2, (PSMB 8.2)	FW: gttccagcatggagtgattg RV: tggttcacccgtaaggcact	77	#86
BiP	FW: catcaagttcttgccgttca RV: tcttcaggagcaaatgtctttgt	99	#10
CHOP/ Gadd153	RV: aaggcactgagcgtatcat FW: tgaagatacacttccttcttgaaca	105	# 21
GAPDH	FW: gctgagtccgcagcagg RV: tgccaacagggagagcaga	78	# 45

Western blotting. To obtain lysates, differentiated SK-N-SH cells (2x 10^5/well in a 12 well plate) were scraped in ice-cold lysis buffer containing 1% Triton X-100 and protease inhibitor cocktail (Roche Applied Science, USA) in PBS. The lysate (supernatant) was obtained after centrifugation at 12 000x g at 4°C for 8 min. Protein concentration was determined with a Bradford protein assay. Equal amounts of protein were analyzed on 8% (BiP, eEF2α), 10% (Ubiquitin) 12% (β2, β2i, β5i) or 18% (LC3) SDS-PAGE gels and blotted onto PVDF membrane (Millipore, USA) using a semi-dry electro blotting apparatus. Blots were pre-incubated with 5% non-fat dried milk in PBS-T (0.05% Tween-20, in PBS) for 1 h and subsequently incubated at 4°C for 16 h with primary antibodies. Membranes were washed 3x for 10 min in PBS-T and subsequently incubated with species specific secondary antibodies conjugated to horseradish peroxidase (dilution 1:2000, Dako, Denmark). Reactive protein bands were visualized using LumiLightPLUS Western blotting substrate (Roche Applied Science, USA) and a LAS-3000 luminescent image analyzer (Fuji Photo Film (Europe), Germany). Results were analyzed using Advanced Image Data Analyzer (AIDA) software (Raytest, Germany) version 3.44.035. The primary antibodies and their dilution factors that were used in this study are listed in Table 2.

Table 2 Primary antibodies and their sources and use.

Antibodies for Western blot analysis				
Antibody	**Species**	**Mono/ polyclonal**	**Dilution**	**Company**
BiP/GRP78	goat	polyclonal	1:1000 in 2.5% milk/ PBS-T	Santa-Cruz, USA
β2	mouse	polyclonal	1:500 in 5% BSA/ PBS-T	Abnova, Taiwan
β2i	mouse	monoclonal	1:500 in 5% BSA/ PBS-T	Abnova, Taiwan
β5i	mouse	monoclonal	1:500 in 5% BSA/ PBS-T	Abnova, Taiwan
LC3	rabbit	polyclonal	1:1000 in 2.5% milk/ PBS-T	Novus Biologicals, USA
Ubiquitin	mouse	monoclonal	1:1000 in 2,5% milk/ PBS-T	Chemicon, USA
eEF2α	rabbit	polyclonal	1:1000 in 2.5% milk/ PBS-T	Cell signal, USA
Antibodies for immunocytochemistry:				
β5i	mouse	monoclonal	1:200 in 1% BSA/ 0.05 % saponin/ PBS-T	Abnova, Taiwan
Calnexin	rabbit	polyclonal	1:200 in 1% BSA/ 0.05% saponin/ PBS-T	Calbiochem/ Merck, Germany
Antibodies for immunohistochemistry				
β2i	mouse	monoclonal	1:100 in 5% BSA/ PBS-T	Abnova, Taiwan
β5i	mouse	monoclonal	1:200 in 5% BSA/ PBS-T	Abnova, Taiwan
pPERK (Thr980)	rabbit	monoclonal	1:1000 in 5% BSA/ PBS-T	Santa Cruz, USA
LC3	rabbit	polyclonal	1:25600 in 5% BSA/ PBS-T or 1: 10000 for double immunohistochemistry	Novus Biologicals, USA
Iba1	rabbit	polyclonal	1:6400 in 5% BSA/ PBS-T	Wako , USA
GFAP	rabbit	polyclonal	1:1800 in 5% BSA/ PBS-T	DAKO, Denmark

Construction of plasmids. The promoter region 500 bp upstream of the transcription start site of the human β2i gene was amplified from human genomic DNA. The promoter sequence was derived from the genomic sequence database *at www.ensembl.org* (NM_002801). Nested PCR was used to maximize the chances of obtaining the correct fragment. The first round of amplification was performed using the primers described in Table 3. A thermocycler was used to

amplify the DNA templates. Reaction volumes of 50 µl contained 1x PCR buffer (Stratagene, USA), 1 mM dNTPs, 2 mM $MgCl_2$, 0.25 µM reverse primer, 0.25 µM forward primer, 0.05 U/µl HotFire Taq polymerase (Stratagene, USA) and 20 µg human genomic DNA. The thermocycler protocol consisted of a 5 min denaturation step at 95°C, amplification was performed using 35 cycles of denaturation (95°C for 45 s), annealing (55°C for 1 min) and elongation (72°C for 1 min). Final extension was performed at 72°C for 8 min. The nested primers used were extended with an *XhoI* or *HindIII* endonuclease site (Table 3). PCR reactions were performed as described above, with the exception of a 1 min denaturing step, in a total reaction volume of 50 µl. The PCR product size was analysed by agarose gel electrophoresis, sequenced and purified using the High Pure PCR Cleanup Micro Kit (Roche Applied Science, USA). The β2i promoter fragment was digested using the restriction enzymes *XhoI* and *HindIII* and subsequently ligated into the pGL3-basic luciferase reporter vector (Promega, USA). The β2i promoter NF-κB binding site was abolished by site-directed mutagenesis using the QuickChange Site Directed Mutagenesis kit (Stratagene, USA), according to the manufacturer's protocol. Three guanines, located in the NF-κB consensus site, were substituted by thymidines, rendering the site nonfunctional. The BiP promoter construct used was previously described.[22]

Table 3 Primers used for subcloning of the β2i promoter. Endonuclease sites are in italics. Mutated nucleotides are indicated in bold.

β2i first round primers	
FW:	5'-TTTAGAAAGACCCGCTCT-3'
RV	5'-GCTAGGCTTCACGTCTGT-3'
Nested primers with endonuclease site	
FW-XhoI:	5'-ATA*CTCGAG*TGGTGCCCTCTTGAGAGA-3'
RV-HindIII	5'-CGC*AAGCTT*GTACTTCCTGCTTTCGCT-3'
Site directed mutagenesis primers	
FW:	5'-AGCACAGAGGGCACAGCAA**TTT**ACATCACCCGGTTCCC-3'
RV:	5'-GGGAACCGGGTGATGT**AAA**TTGCTGTGCCCTCTGTGCT-3'

Promoter activity assay. For transient transfections, HEK 293 cells (10^5 cells/well in a 24 well plate) were transfected using Lipofectamine 2000 (Invitrogen, USA) according to the manufacturer's protocol. One hundred nanograms of DNA of luciferase reporter construct was cotransfected with 1 ng CMV-Renilla construct (Promega, USA). Cells were incubated for 16 h and treated with different concentration of tunicamycin and γIFN for an additional 16 h. Cells were harvested by scraping into 250 µl Passive Lysis Buffer (Promega, USA), vigorous shaking for 15 min and 12 000x g centrifugation at 4°C for 8 min. The sample (20 µl) was incubated with a Renilla or Luciferase substrate (Promega, USA) and luminescence was measured on a GloMax Multi Microplate Multimode Reader (Promega, USA).

Immunocytochemistry. Differentiated SK-N-SH cells were grown ($2x10^5$ cells/well in a 12 well plate) on non-coated sterile glass coverslips. Cells were washed in ice cold PBS and fixed using 4% paraformaldehyde (Sigma, The Netherlands) for 15 min and permeabilized in ice cold (-20 °C) methanol (Merck, Germany) for 5 min. In order to block antibody non-specific binding the cells were incubated in blocking buffer (0.1% bovine serum albumine (BSA, Boehringer, Germany) and 0.05% saponine (in PBS-T, Sigma, The Netherlands) for 30 min at room temperature. Double staining was performed using antibodies directed against β5i and calnexin in blocking buffer at room temperature for 1 h (Table 2). Glass slides were washed in PBS-T and subsequently incubated with species specific secondary antibodies labelled with Cy3 or FITC fluorescent label (dilution 1:200 in blocking buffer, Jackson Immuno Research, USA) for 1 h. Cells were washed in PBS-T and incubated with diamidino phenylindole (DAPI, dilution 1:1000 Sigma, USA) for 5 min. After rinsing in PBS the glass slides were air dried, embedded in vectashield (Vector Laboratories, USA) and mounted onto glass slides. Imaging was performed using a Leica TCS-SP@ mounted on an inverted microscope (Leica, Germany) equipped with a digital CCD camera.

In-gel proteasome activity assay. SK-N-SH cells (10^5 cells/well in a 24 well plate) were differentiated for 7 days before incubation for 16 h in the presence or absence of Tm before addition of Me_4BodipyFL-Ahx$_3$Leu$_3$VS (Me_4BodipyFL probe), a close analogue of the BodipyFL probe described previously,[27] at a concentration of 500 nM for 5 h, followed by a chase for 1 h with MG132. The in-gel proteasome activity assay was performed essentially as described.[27] In short, cells were lysed in ice-cold lysis buffer and equal amounts of protein were separated on a 12.5% SDS-PAGE gel. In-gel visualization of the labelled subunits was performed in the wet gel slabs directly by using the GFP settings (λ_{ex} 480, λ_{em} 510) on the Typhoon Variable Mode Imager (Amersham Biosciences).

Immunohistochemistry. Post-mortem brain material was obtained from the Netherlands Brain Bank (Table 4). Informed consent is available for each patient. Sections (5 µm thick) were mounted on Superfrost plus tissue slides (Menzel-Gläser, Germany) and dried overnight at 37°C. For all stainings sections were deparaffinised and subsequently immersed in 0.3% H_2O_2 in methanol for 30 minutes to quench endogenous peroxidase activity and washed for 5 minutes in PBS. Sections were treated with 10 mmol/L pH 6.0 sodium citrate buffer heated by microwave for 10 minutes for antigen retrieval and subsequently incubated with primary antibodies at 4°C for 16 h. Antibodies (Table 2) were diluted in PBS containing 1% (w/v) bovine serum albumin (BSA, Boehringer Mannheim, Germany). Negative controls for all immunostainings were generated by omission of primary antibodies. Sections were washed 3x for 10 min with PBS and subsequently incubated with horseradish peroxidase labelled α mouse/rabbit secondary antibody (Dako REAL^{TM} EnVision^{TM}/HRP Rabbit/Mouse, Dako, Germany). Colour was developed using 3,3'-diaminobenzidine (0.1 mg/ml, 0.02% H_2O_2, 10 minutes; Sigma,) as chromogen. Sections were counterstained with hematoxylin and mounted using Depex (BDH Laboratories Supplies, UK). For double immunohistochemistry with pPERK and LC3 sections were treated as described above to quench endogenous peroxidase activity and incubated with

the pPERK antibody diluted in PBS containing 1% BSA at room temperature for 1 h. Sections were washed 3x 10 min with PBS and subsequently incubated with horseradish labelled goat-anti-rabbit secondary antibody (Dako, Germany) for 1 h. Sections were washed 3x 10 min with PBS and colour was developed using 3,3'-diaminobenzidine (0.1 mg/ml, 0.02% H_2O_2, 10 minutes; Sigma, USA) as chromogen. Development time was determined using a single antibody control. Sections were washed with water and subsequently treated with 10 mmol/L pH 6.0 sodium citrate buffer heated by autoclave for 10 min for antigen retrieval. Sections were washed with PBS for 5 min, preincubated with normal swine serum (1:10 in 5% BSA/PBS, Dako, Germany) for 10 minutes and incubated with the LC3 antibody at 4°C for 16 h. Sections were washed 3x 10 min with PBS and incubated with biotinylated swine-anti-rabbit (1:300 in 5% BSA/PBS, Dako, Germany) for 1 h. Sections were washed 3x 10 min with PBS and incubated with streptavidin horseradish peroxidase (1:100 in 5% BSA/PBS, Dako, Germany) for 1 h. Sections were washed 3x 10 min with PBS and 1x in Tris – HCL buffer (pH 6.8). Colour was developed using liquid permanent red (LPR, DAKO, Germany). Development time was determined using a single antibody control. Sections were counterstained with hematoxylin and mounted using Aquamount (BDH Laboratories Supplies). A section incubated only with pPERK antibody but developed at the LPR step was used as a cross-reactivity control. Double immunohistochemistry using β5i and GFAP or Iba was performed as described above with minor modifications. Slides were preincubated with normal goat serum (1:10 in 5% BSA/PBS) and incubated with both primary antibodies overnight at 4°C. Sections were washed 3x 10 min with PBS and subsequently incubated with horseradish labelled goat-anti-mouse (undiluted, DAKO, Germany) and biotinylated goat anti rabbit (1:100 in 5% BSA/PBS, DAKO, Germany) antibodies. Slides were washed 3x 10 min in PBS and incubated with streptavidin horseradish peroxidase (1:100 in 5% BSA/PBS, DAKO, Germany) for 1 hr. Sections were washed 3x 10 min in PBS and developed using 3,3'-diaminobenzidine as chromogen. Slides were washed in water and in 1x Tris–HCL buffer before developing with LPR. Sections were counterstained with hematoxylin

and mounted using Aquamount. We used the Nuance spectral imaging system (CRi, USA) to analyze the double stained sections. Spectral libraries of single-brown (DAB), single-red (LPR) and hematoxylin were obtained from control sections. The spectral library was used to unmix the different reactions products in the double stained sections into black and white images. These images represent the localization of each of the reactions products and were reverted to fluorescence-like images composed of pseudo-colours by the Nuance software.

Table 4: Overview of the post-mortem brain material used in this study (CON= control case, MCI=mild cognitive impairment, M=male, F=female, PMI=post-mortem interval).

Case	Braak score for NFT	Braak score for amyloid	Clinical diagnosis	Age	Sex	PMI (h)
1	0	0	CON	57	M	6
2	0	A	CON	66	F	5
3	1	A	CON	82	F	5
4	2	0	CON	78	M	6
5	3	C	MCI	74	M	5
6	3	C	AD	69	F	5
7	4	C	AD	57	F	5
8	5	C	AD	87	M	6
9	6	C	AD	57	M	5
10	6	C	AD	80	F	6

Titles and legends to figures

Figure 1 Expression of β2i and β5i immunoproteasome subunits is increased in AD hippocampus. Representative immunohistochemical stainings for β2i (a-f) and β5i (g-l) in the hippocampal CA1 and CA4 region of a non-demented control Braak 1/0 (CA1 (a,g), CA4 (b,h)), AD Braak 3C (CA1 (c,i), CA4 (d,j)) and AD Braak 5C (CA1 (e,k), CA4 (f,l)) case. Reactivity to β2i is present in neurons, glial and endothelial cells and increases with the Braak stage for NFTs. Double immunolabelling shows β5i expression in astrocytes using GFAP as a marker (m) and microglia using Iba1 as a marker (n) in AD hippocampus. Nuclei were counterstained with hematoxylin (blue). The GFAP/ Iba1 and β5i signals were spectrally unmixed and are shown separately (m/n 1 and m/n 2, respectively) and as a merge with artificial colours (m/n 3: GFAP/Iba1: red; β5i: green). Scale bar: 50 μM.

Figure 2 Effects of ER stress on proteasome β subunit expression. Differentiated SK-N-SH cells were treated with γIFN or Tm for 16 h. Relative mRNA and protein levels of proteasome subunits were determined using quantitative PCR and Western blotting. (a) Normalized mRNA expression levels of the proteasome subunits α (HC5 and C7) and β (β1, -2, -5, -2i and -5i) and (b) ER stress responsive genes BiP and CHOP. Expression levels were normalized to GAPDH mRNA levels. Data are mean ± SD from triplicate observations of a representative experiment. Asterisks indicate significant differences compared to control levels ($p < 0.05$). (c) Western blot analysis with antibodies directed against the β5i, β2i and β2 subunits and the ER stress responsive protein BiP. Asterisk indicates cross reactivity of the BiP antibody with Hsc70. The expression levels of eEF2α are indicated as loading control. Shown are blots from a representative experiment.

Figure 3 ER stress does not increase β5i promoter activity. (a) Representation of binding sites for ER stress responsive transcription factors in the promoter regions of the β subunits of the proteasome. No classical ERSE binding motifs are identified; in contrast putative NF-κB (p50-p65) binding sites are present in the proximal promoter region of all the immuno β subunits. The location of the binding site is indicated relative to the transcription start site. (b) Relative activity of β5i, β5i NF-κB binding site mutant (β5i ΔNF-κB) and BiP promoters in Hek293 cells. Promoter activities were determined using a luciferase-renilla assay as described in the materials and methods section in the presence or absence of γIFN or Tm at the indicated concentrations for 16

h. Data are mean ± SD from triplicate observations of a representative experiment. Asterisks indicate significant differences compared to control ($p < 0.05$)

Figure 4 ER stress does not influence β5i localization. Differentiated SK-N-SH cells were treated with γIFN or Tm for 16 h at the indicated concentrations compared to a non-treated control. Shown are confocal pictures of the localization of β5i (left hand panel) and calnexin (middle panel) by immunofluorescence. An overlay of β5i (red), calnexin (green) and DAPI nuclear counterstain (blue) is shown on the right. Scale bar: 20 μM.

Figure 5 ER stress does not increase proteasome activity. Differentiated SK-N-SH cells were treated with indicated concentrations of Tm for 16 h and incubated with the Me_4BodipyFL proteasome activity probe for 5 h. (a) Visualization of probe binding after SDS-PAGE using a 2D proteomic imaging system shows probe binding to the β2 and β5 subunits predominantly (activity). The lower panel is a Western blot of the same samples showing that β2 expression levels are not changed by the treatment (protein). (b) Quantification of the fluorescence intensity of the bands in the upper panel of (a), corrected for loading by the expression levels of eEF2α (not shown) and presented as % of untreated control cells. This reflects the relative activity of the β2 and β5 subunits following Tm treatment.

Figure 6 ER stress induces autophagy and does not lead to increased polyubiquitination. Differentiated SK-N-SH cells were treated with ER stressors (Tm, Th and 2DG), γIFN and the proteasome inhibitor epoxomycin for 16 h and protein levels were analysed by Western blotting. (a) Blots showing changes in the level of ubiquitinated (Ub) proteins (upper panel) and LC3-I and LC3-II (middle panel) following treatment with ER stressors, γIFN and epoxomycin. The expression levels of eEF2α are indicated as loading control. Shown are blots from a representative experiment. (b) LC3-II/LC3-I ratios determined from (a).

Figure 7 LC3 levels are increased in pPERK positive neurons in the AD hippocampus. (a) Immunohistochemistry showing LC3 levels in hippocampal neurons of a representative AD (Braak 4C) case. Shown is a part of the CA1 and subiculum (sub) area. Scale bar: 500 μM. (b, c) Magnification of CA1 (b) and subiculum (c) from (a), showing LC3 levels are increased in neurons with GVD. (d) Representative double immunohistochemistry staining showing LC3 levels are increased in neurons that show pPERK reactivity. Nuclei were counterstained with hematoxylin (blue). The LC3 and pPERK signals were spectrally unmixed and are shown

separately (d1 and 2, respectively) and as a merge with artificial colours (d3: LC3 red; pPERK green). Scale bar (b–c) 25 μM.

Figure 8 ER stress preferentially activates autophagy in neuronal cells. (a) Diagram showing the pathways investigated in this study by which ER stress may increase the proteolytic capacity of neuronal cells. ER stress could enhance proteolytic degradation by the proteasome by influencing the subunit composition via activation of the EOR. Alternatively the UPR can be employed to enhance the expression levels of the constitutive subunits. In addition, regulation of the localization or activity of the proteasome may occur. In addition the UPR may result in activation of autophagy. (b) Our data show that a disturbance of ER homeostasis resulting in activation of the UPR will activate the autophagy pathway. This can be due to a decreased capability to export misfolded proteins from the ER lumen under these conditions or may relate to the inability of the proteasome to degrade aggregated proteins. In AD neurons, decreased proteasomal degradation as well as a disruption in the autophagosomal/lysosomal system may eventually lead to neurodegeneration.

Reference List

1. Braak H and Braak E (1995) Staging of Alzheimer's disease-related neurofibrillary changes. Neurobiol. Aging 16:271-278

2. Hoozemans JJM, van Haastert ES, Nijholt DAT, Rozemuller AJM, Eikelenboom P and Scheper W (2009) The Unfolded Protein Response Is Activated in Pretangle Neurons in Alzheimer's Disease Hippocampus. American Journal of Pathology 174:1241-1251

3. Hoozemans JJM, Veerhuis R, van Haastert ES, Rozemuller JM, Baas F, Eikelenboorn P and Scheper W (2005) The unfolded protein response is activated in Alzheimer's disease. Acta Neuropathologica 110:165-172

4. Meyer M, Caselmann WH, Schluter V, Schreck R, Hofschneider PH and Baeuerle PA (1992) Hepatitis B virus transactivator MHBst: activation of NF-kappa B, selective inhibition by antioxidants and integral membrane localization. EMBO J. 11:2991-3001

5. Pahl HL and Baeuerle PA (1995) A novel signal transduction pathway from the endoplasmic reticulum to the nucleus is mediated by transcription factor NF-kappa B. EMBO J. 14:2580-2588

6. Hoseki J, Ushioda R and Nagata K (2010) Mechanism and components of endoplasmic reticulum-associated degradation. J. Biochem. 147:19-25

7. Yoshida H, Matsui T, Hosokawa N, Kaufman RJ, Nagata K and Mori K (2003) A time-dependent phase shift in the mammalian unfolded protein response. Dev. Cell 4:265-271

8. Pickart CM and Cohen RE (2004) Proteasomes and their kin: proteases in the machine age. Nat. Rev. Mol. Cell Biol. 5:177-187

9. Cardozo C and Michaud C (2002) Proteasome-mediated degradation of tau proteins occurs independently of the chymotrypsin-like activity by a nonprocessive pathway. Archives of Biochemistry and Biophysics 408:103-110

10. Cecarini V, Ding Q and Keller JN (2007) Oxidative inactivation of the proteasome in Alzheimer's disease. Free Radic. Res. 41:673-680

11. Keller JN, Hanni KB and Markesbery WR (2000) Impaired proteasome function in Alzheimer's disease. J. Neurochem. 75:436-439

12. McNaught KS, Bjorklund LM, Belizaire R, Isacson O, Jenner P and Olanow CW (2002) Proteasome inhibition causes nigral degeneration with inclusion bodies in rats. Neuroreport 13:1437-1441

13. Mishto M, Bellavista E, Santoro A, Stolzing A, Ligorio C, Nacmias B, Spazzafumo L, Chiappelli M, Licastro F, Sorbi S, Pession A, Ohm T, Grune T and Franceschi C (2006) Immunoproteasome and LMP2 polymorphism in aged and Alzheimer's disease brains. Neurobiology of Aging 27:54-66

14. Drews O, Wildgruber R, Zong C, Sukop U, Nissum M, Weber G, Gomes AV and Ping P (2007) Mammalian proteasome subpopulations with distinct molecular compositions and proteolytic activities. Mol. Cell Proteomics. 6:2021-2031

15. Yorimitsu T, Nair U, Yang Z and Klionsky DJ (2006) Endoplasmic reticulum stress triggers autophagy. J. Biol. Chem. 281:30299-30304

16. Ogata M, Hino S, Saito A, Morikawa K, Kondo S, Kanemoto S, Murakami T, Taniguchi M, Tanii I, Yoshinaga K, Shiosaka S, Hammarback JA, Urano F and Imaizumi K (2006) Autophagy is activated for cell survival after endoplasmic reticulum stress. Mol. Cell Biol. 26:9220-9231

17. Ding WX, Ni HM, Gao W, Yoshimori T, Stolz DB, Ron D and Yin XM (2007) Linking of autophagy to ubiquitin-proteasome system is important for the regulation of endoplasmic reticulum stress and cell viability. Am. J. Pathol. 171:513-524

18. Hara T, Nakamura K, Matsui M, Yamamoto A, Nakahara Y, Suzuki-Migishima R, Yokoyama M, Mishima K, Saito I, Okano H and Mizushima N (2006) Suppression of basal autophagy in neural cells causes neurodegenerative disease in mice. Nature 441:885-889

19. Komatsu M, Waguri S, Chiba T, Murata S, Iwata J, Tanida I, Ueno T, Koike M, Uchiyama Y, Kominami E and Tanaka K (2006) Loss of autophagy in the central nervous system causes neurodegeneration in mice. Nature 441:880-884

20. Boland B, Kumar A, Lee S, Platt FM, Wegiel J, Yu WH and Nixon RA (2008) Autophagy induction and autophagosome clearance in neurons: relationship to autophagic pathology in Alzheimer's disease. J. Neurosci. 28:6926-6937

21. Okamoto K, Hirai S, Iizuka T, Yanagisawa T and Watanabe M (1991) Reexamination of granulovacuolar degeneration. Acta Neuropathol. 82:340-345

22. Kap YS, Hoozemans JJM, Bodewes AJ, Zwart R, Meijer OC, Baas F and Scheper W (2007) Pin1 levels are downregulated during ER stress in human neuroblastoma cells. Neurogenetics 8:21-27

23. Brooks P, Murray RZ, Mason GG, Hendil KB and Rivett AJ (2000) Association of immunoproteasomes with the endoplasmic reticulum. Biochem. J. 352 Pt 3:611-615

24. Palmer A, Rivett AJ, Thomson S, Hendil KB, Butcher GW, Fuertes G and Knecht E (1996) Subpopulations of proteasomes in rat liver nuclei, microsomes and cytosol. Biochem. J. 316 (Pt 2):401-407

25. Reits EA, Benham AM, Plougastel B, Neefjes J and Trowsdale J (1997) Dynamics of proteasome distribution in living cells. EMBO J. 16:6087-6094

26. Menendez-Benito V, Verhoef LG, Masucci MG and Dantuma NP (2005) Endoplasmic reticulum stress compromises the ubiquitin-proteasome system. Hum. Mol. Genet. 14:2787-2799

27. Verdoes M, Florea BI, Menendez-Benito V, Maynard CJ, Witte MD, van der Linden WA, van den Nieuwendijk AM, Hofmann T, Berkers CR, Van Leeuwen FW, Groothuis TA, Leeuwenburgh MA, Ovaa H, Neefjes JJ, Filippov DV, van der Marel GA, Dantuma NP and Overkleeft HS (2006) A fluorescent broad-spectrum proteasome inhibitor for labeling proteasomes in vitro and in vivo. Chem. Biol. 13:1217-1226

28. Chafekar SM, Hoozemans JJ, Zwart R, Baas F and Scheper W (2007) Abeta 1-42 induces mild endoplasmic reticulum stress in an aggregation state-dependent manner. Antioxid. Redox Signal 9:2245-2254

29. Yorimitsu T and Klionsky DJ (2007) Endoplasmic reticulum stress: a new pathway to induce autophagy. Autophagy 3:160-162

30. Mizushima N and Yoshimori T (2007) How to interpret LC3 immunoblotting. Autophagy 3:542-545

31. Diaz-Hernandez M, Hernandez F, Martin-Aparicio E, Gomez-Ramos P, Moran MA, Castano JG, Ferrer I, Avila J and Lucas JJ (2003) Neuronal induction of the immunoproteasome in Huntington's disease. Journal of Neuroscience 23:11653-11661

32. Puttaparthi K and Elliott JL (2005) Non-neuronal induction of immunoproteasome subunits in an ALS model: possible mediation by cytokines. Exp. Neurol. 196:441-451

33. Diaz-Hernandez M, Martin-Aparicio E, Avila J, Hernandez F and Lucas JJ (2004) Enhaced induction of the immunoproteasome by interferon gamma in neurons expressing mutant Huntingtin. Neurotoxicity Research 6:463-468

34. Godbout JP and Johnson RW (2004) Interleukin-6 in the aging brain. J. Neuroimmunol. 147:141-144

35. Akiyama H, Barger S, Barnum S, Bradt B, Bauer J, Cole GM, Cooper NR, Eikelenboom P, Emmerling M, Fiebich BL, Finch CE, Frautschy S, Griffin WS, Hampel H, Hull M, Landreth G, Lue L, Mrak R, Mackenzie IR, McGeer PL, O'Banion MK, Pachter J, Pasinetti G, Plata-Salaman C, Rogers J, Rydel R, Shen Y, Streit W, Strohmeyer R, Tooyoma I, Van Muiswinkel FL, Veerhuis R, Walker D, Webster S, Wegrzyniak B, Wenk G and Wyss-Coray T (2000) Inflammation and Alzheimer's disease. Neurobiol. Aging 21:383-421

36. Kaltschmidt B, Uherek M, Volk B, Baeuerle PA and Kaltschmidt C (1997) Transcription factor NF-kappaB is activated in primary neurons by amyloid beta peptides and in neurons surrounding early plaques from patients with Alzheimer disease. Proc. Natl. Acad. Sci. U. S. A 94:2642-2647

37. Gillardon F, Kloss A, Berg M, Neumann M, Mechtler K, Hengerer B and Dahlmann B (2007) The 20S proteasome isolated from Alzheimer's disease brain shows post-translational modifications but unchanged proteolytic activity. J. Neurochem. 101:1483-1490

38. Gregori L, Fuchs C, Figueiredo-Pereira ME, Van Nostrand WE and Goldgaber D (1995) Amyloid beta-protein inhibits ubiquitin-dependent protein degradation in vitro. J. Biol. Chem. 270:19702-19708

39. Mizushima N, Yamamoto A, Matsui M, Yoshimori T and Ohsumi Y (2004) In vivo analysis of autophagy in response to nutrient starvation using transgenic mice expressing a fluorescent autophagosome marker. Mol. Biol. Cell 15:1101-1111

40. Tan JM, Wong ES, Kirkpatrick DS, Pletnikova O, Ko HS, Tay SP, Ho MW, Troncoso J, Gygi SP, Lee MK, Dawson VL, Dawson TM and Lim KL (2008) Lysine 63-linked ubiquitination promotes the formation and autophagic clearance of protein inclusions associated with neurodegenerative diseases. Hum. Mol. Genet. 17:431-439

41. Pickford F, Masliah E, Britschgi M, Lucin K, Narasimhan R, Jaeger PA, Small S, Spencer B, Rockenstein E, Levine B and Wyss-Coray T (2008) The autophagy-related protein beclin 1 shows reduced expression in early Alzheimer disease and regulates amyloid beta accumulation in mice. J. Clin. Invest 118:2190-2199

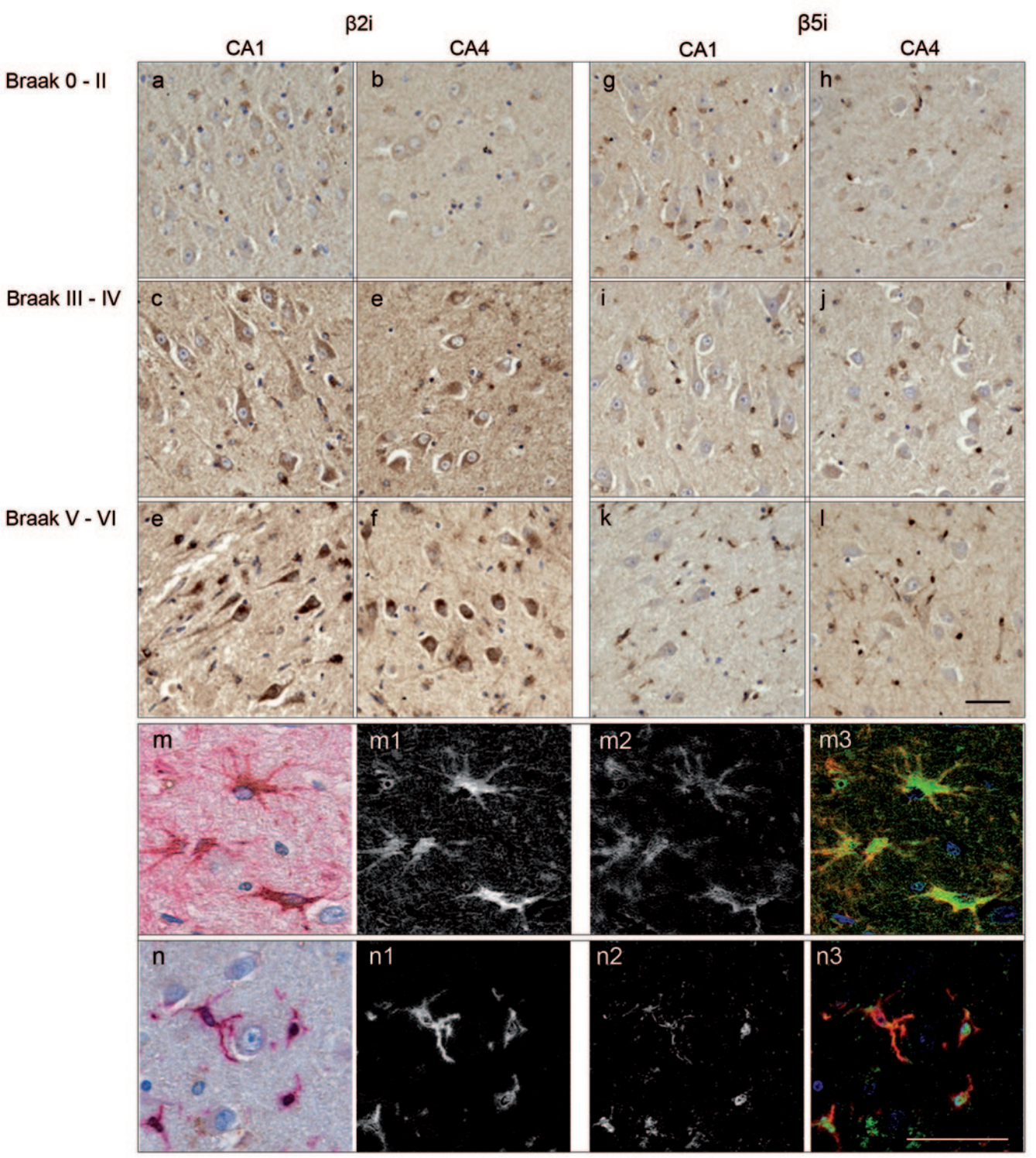
β2i
β5i
CA1
CA4
CA1
CA4
Braak 0 - II
Braak III - IV
Braak V - VI
a
b
g
h
c
e
i
j
e
f
k
l
m
m1
m2
m3
n
n1
n2
n3

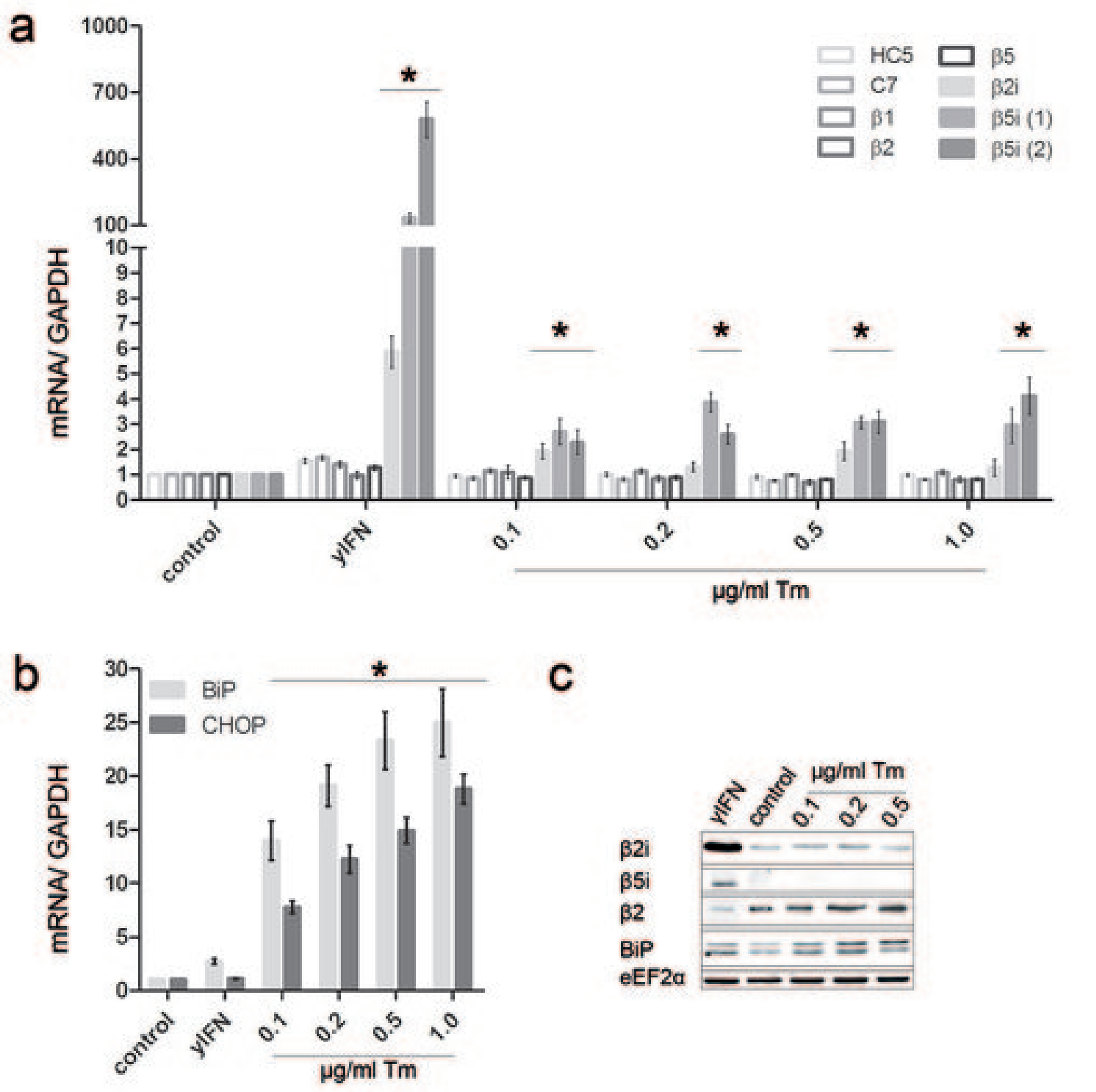
a
mRNA/ GAPDH
HC5
C7
β1
β2
β5
β2i
β5i (1)
β5i (2)
control
γIFN
0.1
0.2
0.5
1.0
μg/ml Tm
b
BiP
CHOP
mRNA/ GAPDH
control
γIFN
0.1
0.2
0.5
1.0
μg/ml Tm
c
γIFN
control
μg/ml Tm
0.1
0.2
0.5
β2i
β5i
β2
BiP
eEF2α

a

20S β-type subunit	Human gene	ERSE binding motif	NF-κB binding motif	Location
β1	PSMB6	None	None	
β2	PSMB7	None	None	
β5	PSMB5	None	None	
β1i	PSMB9	None	5′ GGGCTTTTGA 3′	-211
β2i	PSMB10	None	5′ GGGGCTTGCC 3′	-123
β5i	PSMB8	None	5′ GGGACATCAC 3′	-124

b

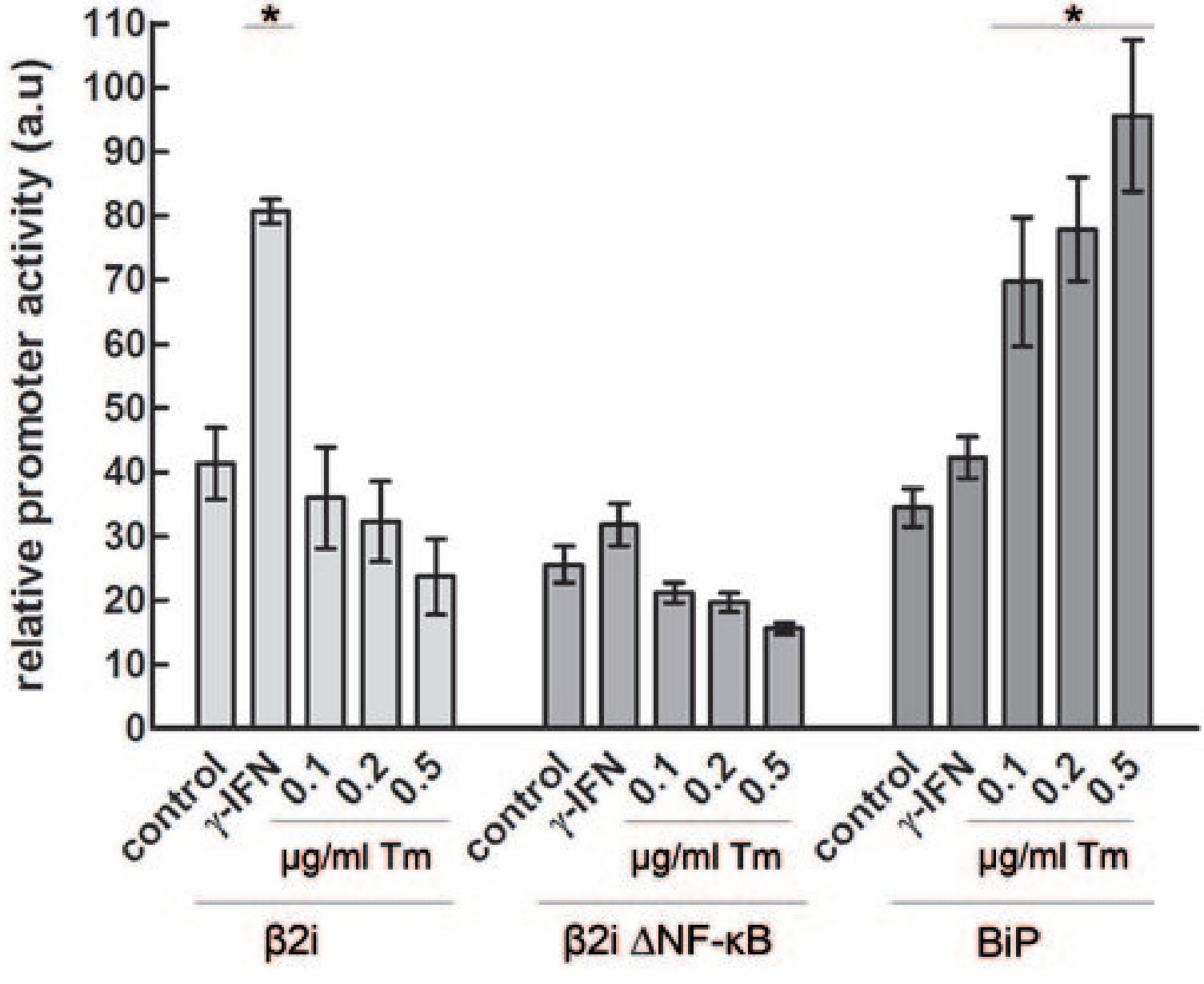

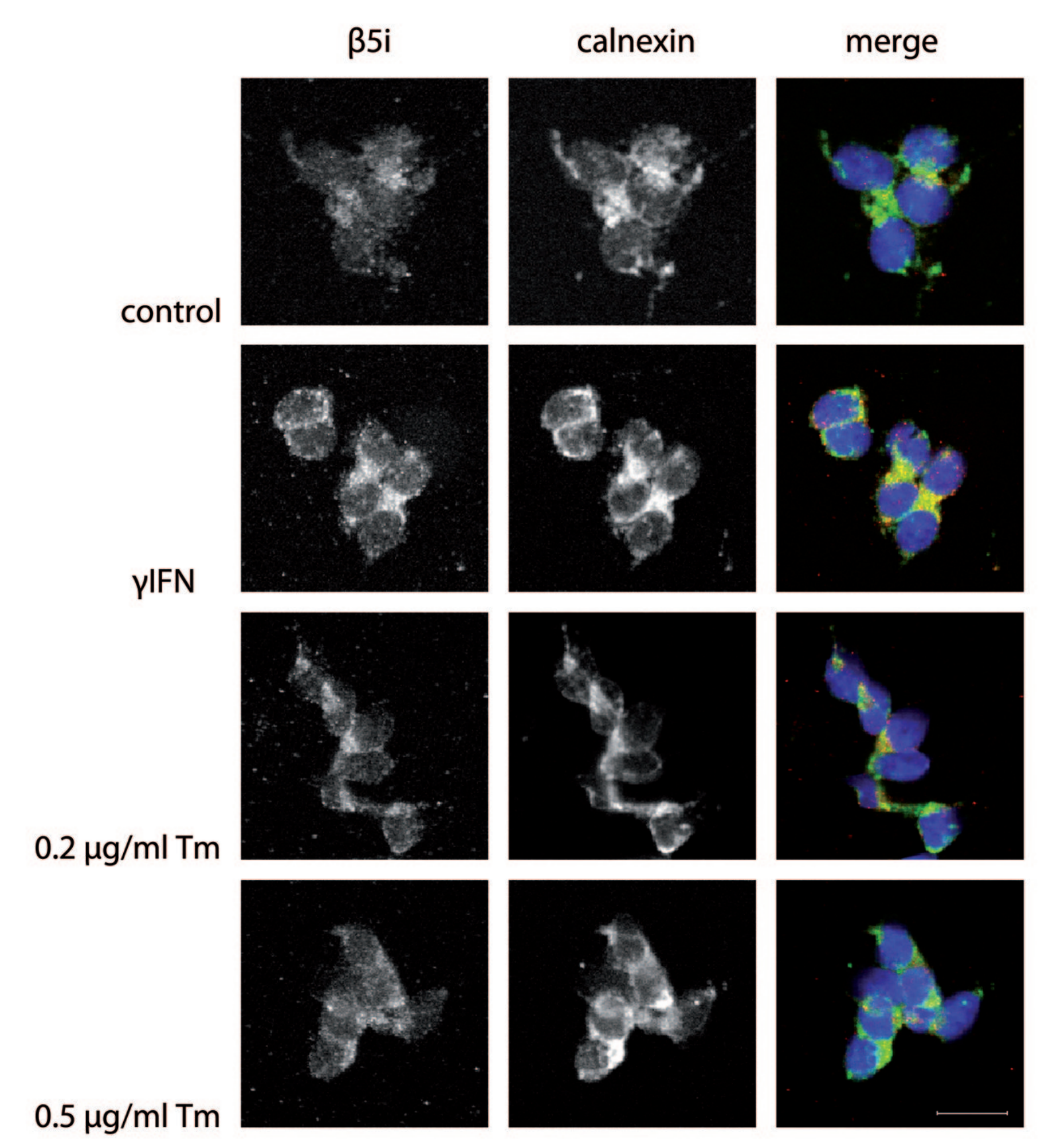
β5i
calnexin
merge
control
γIFN
0.2 µg/ml Tm
0.5 µg/ml Tm

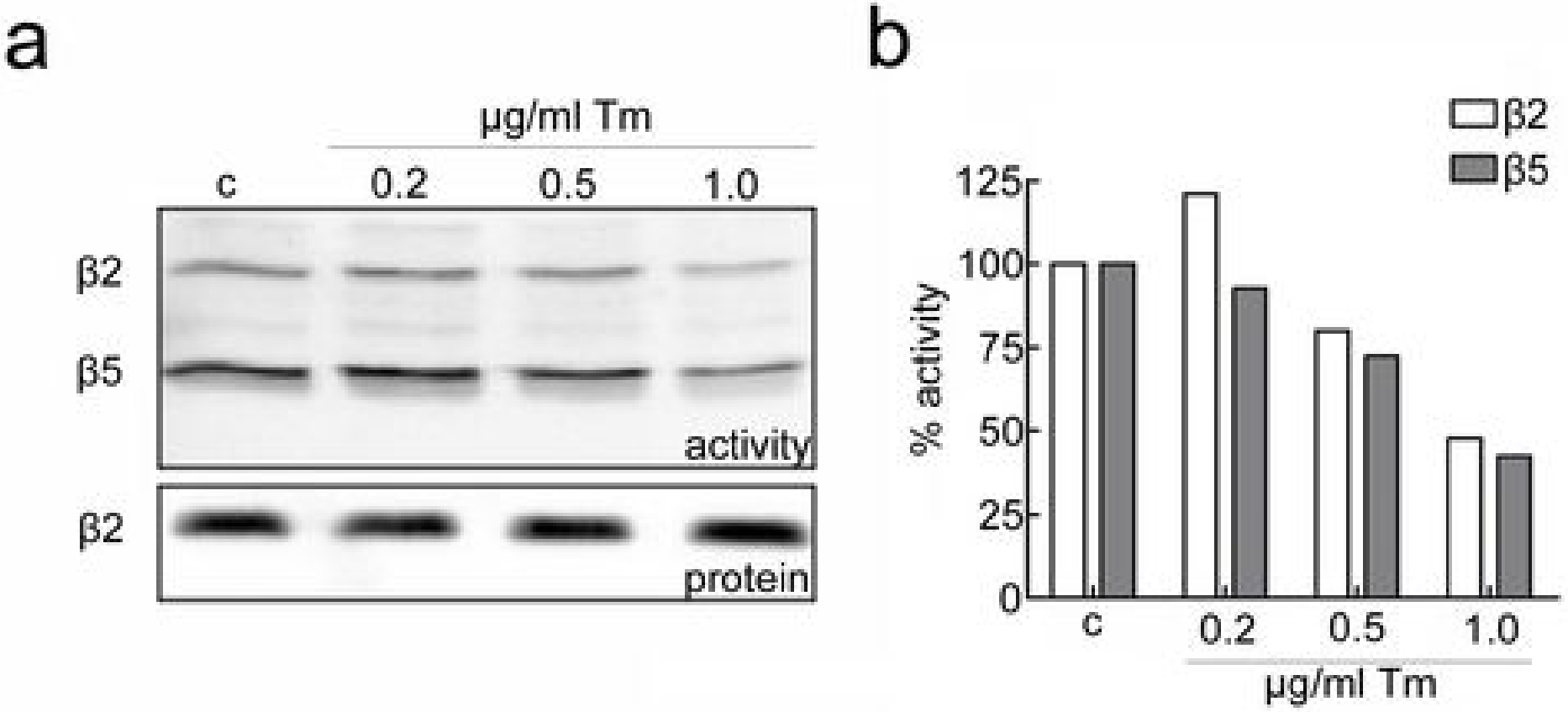
a
µg/ml Tm
c
0.2
0.5
1.0
β2
β5
activity
β2
protein
b
β2
β5
125
100
75
50
25
0
% activity
c
0.2
0.5
1.0
µg/ml Tm

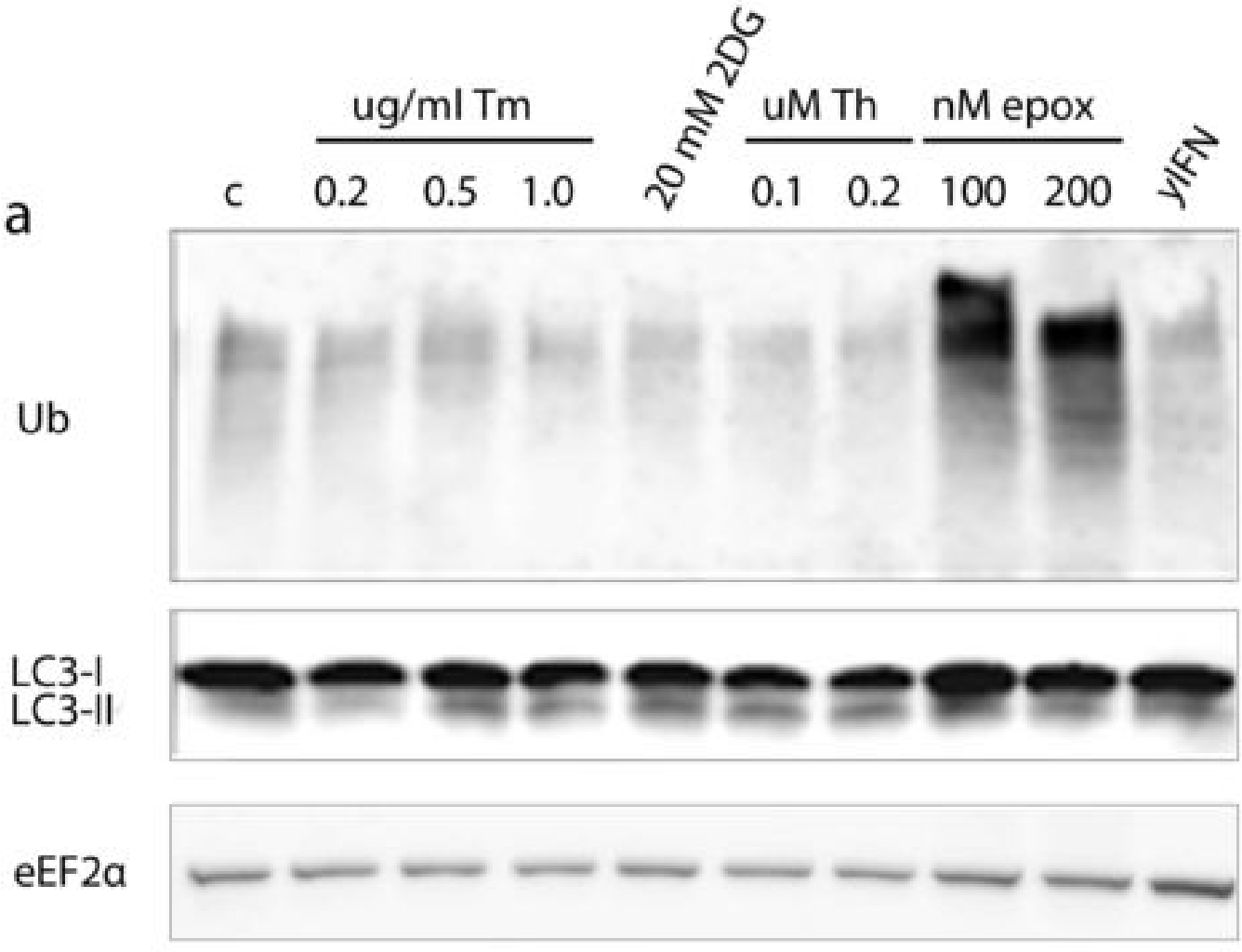
a
ug/ml Tm
20 mM 2DG
uM Th
nM epox
c
0.2
0.5
1.0
0.1
0.2
100
200
γIFN
Ub
LC3-I
LC3-II
eEF2α

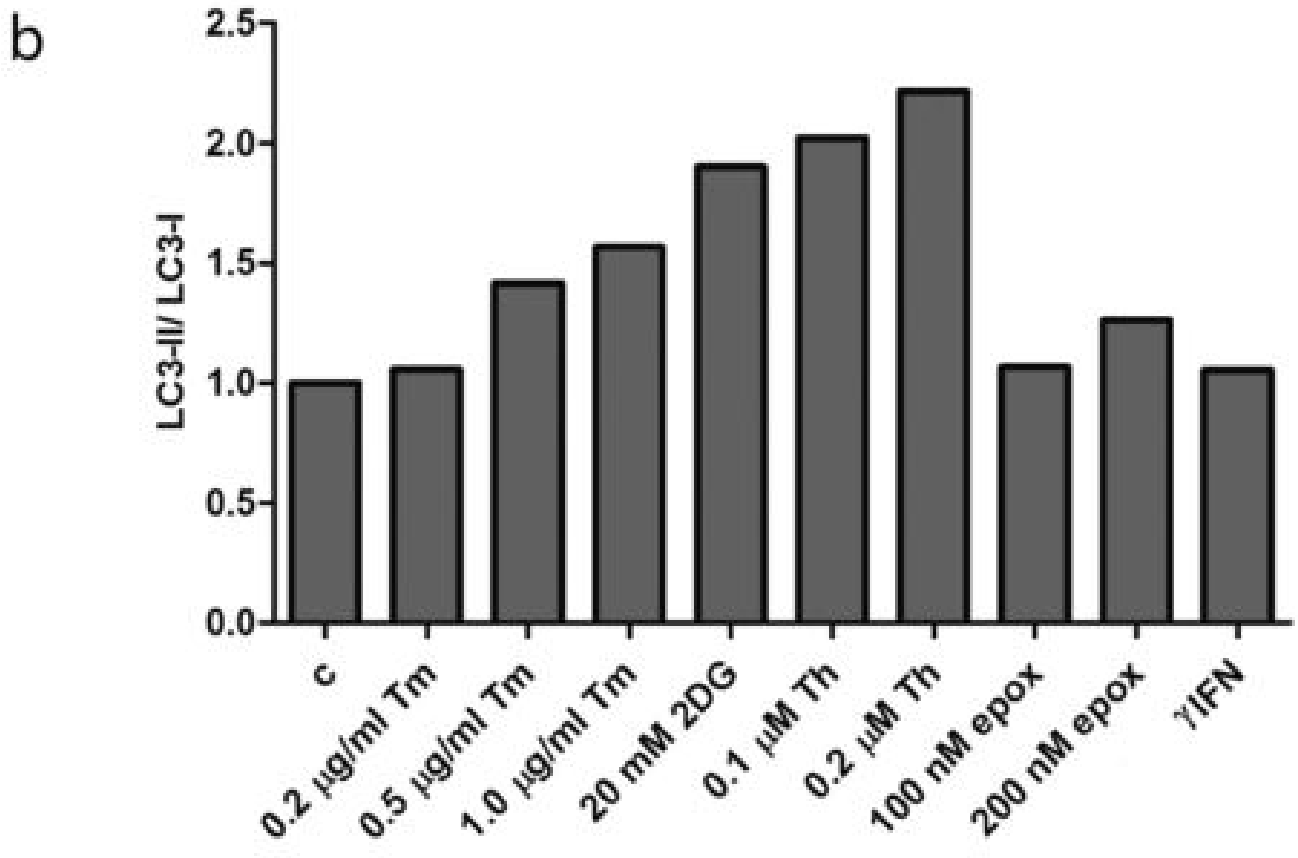
b
LC3-II/ LC3-I
2.5
2.0
1.5
1.0
0.5
0.0
c
0.2 μg/ml Tm
0.5 μg/ml Tm
1.0 μg/ml Tm
20 mM 2DG
0.1 μM Th
0.2 μM Th
100 nM epox
200 nM epox
γIFN

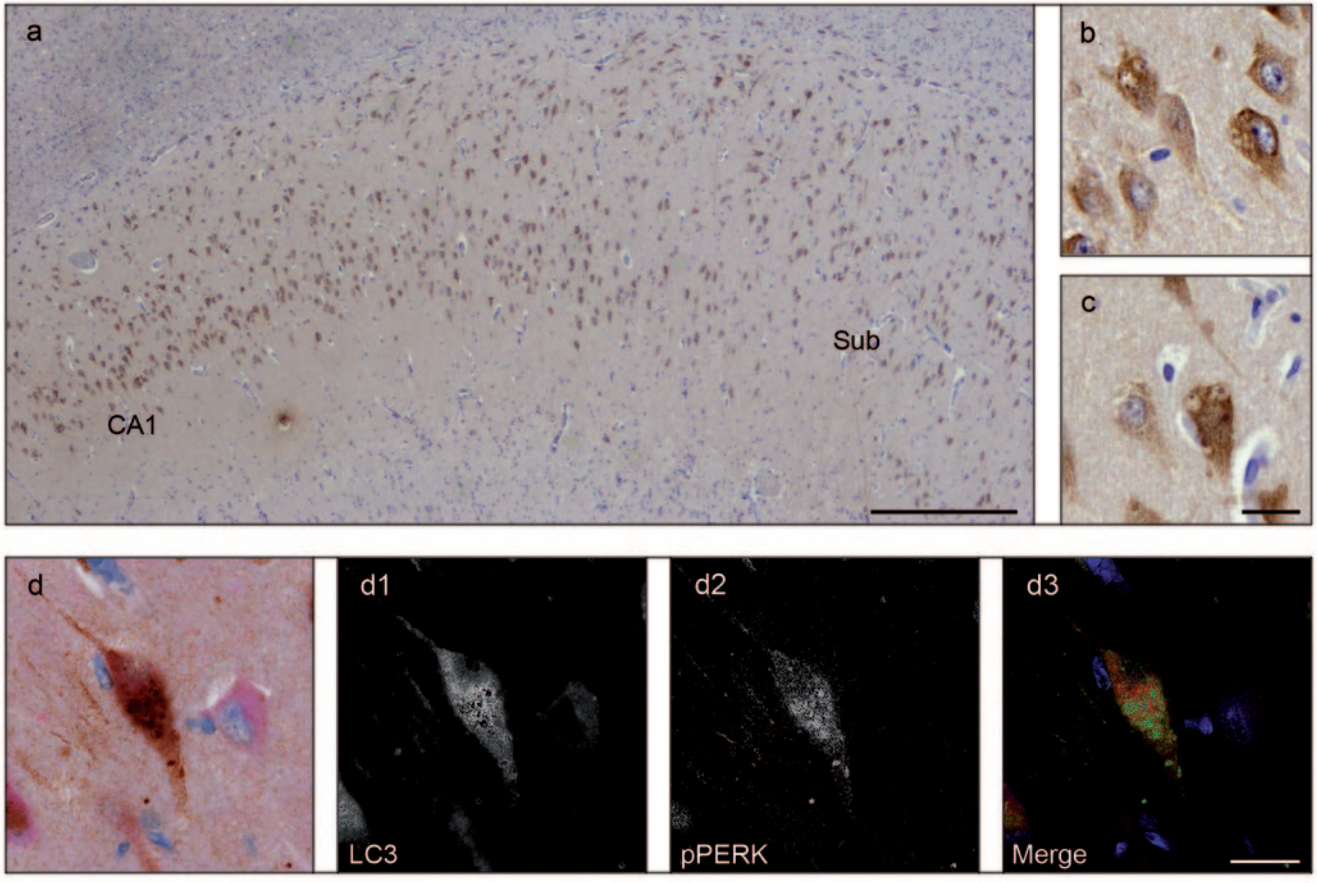
a
b
c
Sub
CA1
d
d1
d2
d3
LC3
pPERK
Merge

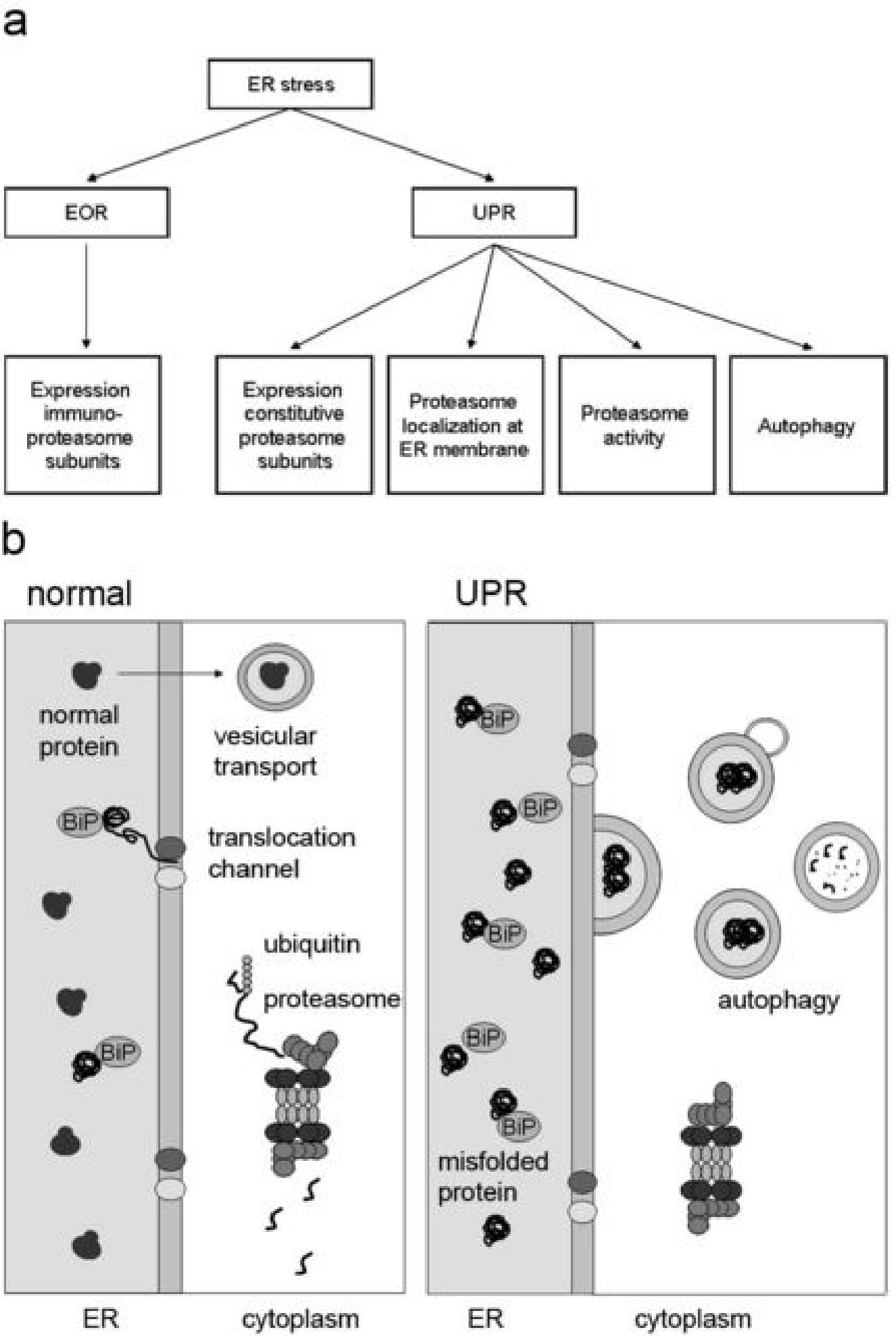
a
ER stress
EOR
UPR
Expression immuno-proteasome subunits
Expression constitutive proteasome subunits
Proteasome localization at ER membrane
Proteasome activity
Autophagy
b
normal
UPR
normal protein
vesicular transport
BiP
translocation channel
ubiquitin
proteasome
BiP
BiP
BiP
BiP
BiP
misfolded protein
autophagy
ER
cytoplasm
ER
cytoplasm